Assessment of Atmosphere-Ocean General Circulation Model Simulations of Northern Hemisphere Atmospheric Blocking

Jessica Vial and Tim Osborn

CLIMATIC RESEARCH UNIT UNIVERSITY OF EAST ANGLIA NORWICH UK

Introduction

Atmospheric blocking are large-scale, quasi-stationary and persistent anticyclones that block or deflect the progression of transient smaller-scale weather systems. They are often responsible for temperature and rainfall anomalies, and sometimes lead to extreme weather events.
In summer 2003, a heat wave developed during a strong and persistent blocking high located over western Europe. This event caused the death of 35.000 people, an economic loss of several million Euros mainly due to a deficit in agricultural production, and severe environmental damage such as forest fires due to extremely high temperatures (De Bono et al., 2004).

The ability of six coupled atmosphere-ocean general circulation models (AOGCM) to simulate the frequency and the duration of atmospheric blocking in the Northern Hemisphere is assessed.
It will contribute to increase our understanding of the mechanisms responsible for the formation and the maintenance of atmospheric blocking, and its impact on extreme weather events. It will also help to indicate the confidence that we have in future projections of extreme weather events that are often the product of large-scale weather regimes such as blocking.

Blocking index and data

During blocking conditions, there are positive geopotential anomalies at high latitudes and negative anomalies at lower latitudes, so that an average easterly flow prevails in the blocked region.
A similar index to the one developed by Tibaldi and Molteni (1990), is used in this study to identify blocking highs in the midlatitudes.
This index measures the strength of the average westerly flow between low (~40˚N) and high (~60˚N) latitudes. Blocking highs also require some time persistence and longitudinal extension. So a large-scale blocking event is defined when the index identifies a blocking-like pattern for three or more adjacent longitudes and during at least five days. A prominent change brought to this index was the use of a central blocking latitude that follows the storm tracks.

The blocking index and subsequent analysis were applied to daily averaged 500 hPa geopotential fields from September 1957 to August 1999.
The models involved in this study are part of the ENSEMBLES project, and contributed to the IPCC AR4 assessment. ERA-40 is the reanalysis dataset used for comparison.

Winter blocking frequency

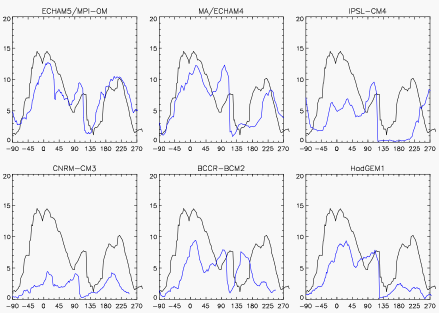

Figure 1: Large-scale winter blocking frequency (%, y-axis) as a function of longitude (x-axis) for ERA-40 (black line) and the model simulations (blue line).

Three main sectors for blocking development are identified by both the reanalysis and the models:

Euro-Atlantic	90˚ W - 45˚ E
Siberia	45˚ E - 110˚ E
Pacific	160˚ E - 240˚ E

The wide range of blocking behaviours is representative of the various modelling techniques employed by the AOGCMs. But the general tendency of the models is to underestimate blocking frequency in the Euro-Atlantic and the Pacific sectors, while most of the AOGCMs overestimate the frequency of Siberian blocking.

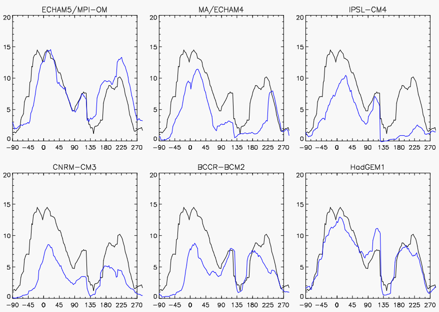

Figure 2: Same as figure 1 after substraction of the time-average systematic error (SE) from the daily 500 hPa geopotential field.

Most of the models simulate the frequency of blocking better when the time-mean bias is removed, but large errors in the variability of the flow are apparently also responsible for discrepancies in blocking frequency.

Atmospheric blocking might be the result of stationary wave amplification, in which case a good simulation of the processes responsible for the time-mean state and the variability in the geopotential field would be essential for the representation of blocking.
To analyse separately the impact of time-mean and variability biases on blocking frequency, the blocking index was applied to a corrected geopotential field (the time-mean systematic error was substracted from daily fields).

In the next section, an EOF analysis previously applied for studying blocking by Ferranti et al. (1994), is performed to assess the ability of the models to simulate the processes responsible for the stationary wave amplification which in turn eventually lead to blocking onset. Processes such as the intensity of the westerlies, the tendency of a split flow and synoptic-eddy activity will be considered for the Euro-Atlantic sector.

EOF analysis of the winter zonal flow

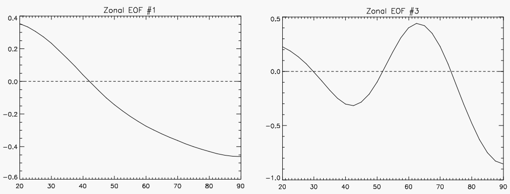

Figure 3: Pattern of the first and third zonal EOFs derived from ERA-40.

	ERA-40		CNRM-CM3		BCCR-BCM2		ECHAM5/MPI-OM		MA/ECHAM4		IPSL-CM4		HadGEM1	
EOF 1	959	129	1095	105	976	115	917	133	974	129	1003	121	963	132
EOF 3	37.4	112	1.9	72	27.4	77	28.5	102	32.5	93	-8.0	92	0.4	110

Table 2: Mean (left) and standard deviation (right) of the zonal EOF coefficients (units are in meters). The simulated fields are projected on the set of EOFs derived from ERA-40. Results for the Euro-Atlantic sector only are shown.

The first zonal EOF shows the height gradient between the tropics and the North Pole. Its coefficients represent the latitudinal average strength of the westerly flow.
Apart from ECHAM5, all models overestimate the average intensity of the westerly flow (Table 2). The temporal variability is in general underestimated except for ECHAM5 and HadGEM1 for which the skewness of the distribution (not shown) indicates more variability towards low values, as compared to ERA-40, which is favourable for blocking development.

The third zonal EOF represents a tendency towards the split of the jet between 40 ˚ N and 60 ˚ N if its coefficients are positive. Negative coefficients are associated with the concentration of the jet around 55 ˚ N.
For all models, underestimation of both the mean and the standard deviation tend the reduce the frequency of occurrence of the split of the flow.

The pattern of second zonal EOF (not shown) shows a positive height gradient south of 50 ˚ N and a negative gradient northward. It represents the position of the jet stream.

Only the first and third EOF patterns show relatively high correlation for both the reanalysis and the models (not shown).
Blocking highs tend to develop for high values of EOF 3 and low values of EOF 1. In other words, both a split and a reduced intensity of the westerly flow are required for blocking onset.

Blocking duration

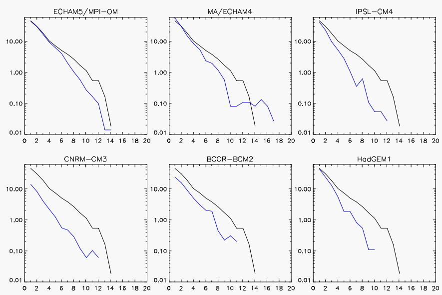

Figure 4: Distribution of the number of winter blocking events (y-axis, log scale) in the Euro-Atlantic region as a function of their duration (days, x-axis) for ERA-40 (black line) and for the model simulations (blue line).

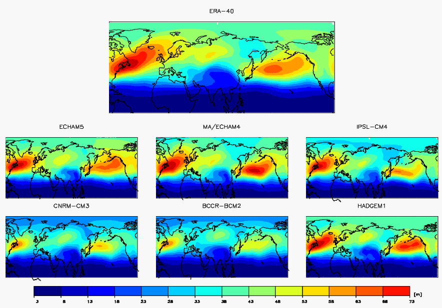

Figure 5: Winter storm track – standard deviation of high-pass filtered 500 hPa geopotential height.

The general tendency of the models is to reproduce shorter blocks than in the reanalysis, except for ECHAM5 and ECHAM4 (Figure 4).
An important process for blocking onset and maintenance, first described by Green (1977) is the straining mechanism of the baroclinic eddies embedded in the main storm tracks.
As they approach the block (in the region of the splitting of the jet), transient eddies are meridionally elongated and zonally compressed, to finally split into two branches that move northward or southward around the block. This deformation of the synoptic-scale eddies by the large-scale flow act to decelerate the westerlies, or even induce an easterly flow, which contributes to maintain the block.

So the lack of eddy activity embedded in the storm track and the reduced amplitude of the split jet might be the cause of the simulated shorter blocks.

ECHAM5 and ECHAM4 are the only models with relatively high eddy activity (Figure 5) and large amplitude of the split jet (Table 2), though still underestimated compared to ERA-40.

Future work

Relationships between blocking and extreme temperature and precipitation events will be analysed for the reanalysis and the AOGCMs, in order to increase our understanding of the impact of blocking on climate extremes. The frequency, duration and geographical patterns of the events will be considered for each blocking sector of the northern hemisphere.
Future projections of blocking and blocking-related extreme weather events will then be investigated under SRES emission scenarios of the IPCC.

References

Ferranti L., Molteni F., Brankovic C., Palmer T.N., (1994) Diagnosis of extratropical variability in seasonal integrations of the ECMWF model. Journal of Climate 7: 849-868
Green J. S. A. (1977) The weather during July 1976: some dynamical considerations of the drought. Weather 32: 120-128
Tibaldi S., Molteni F. (1990) On the operational predictability of blocking. Tellus 42A: 343-365
De Bono A., Giuliani G., Kluser S., Peduzzi P. (March 2004) United Nations Environment Programme (UNEP)

Acknowledgements

The AOGCMs data are provided by the CERA database which is run by the Model and Data group at the Max-Planck-Institute for Meteorology. ERA-40 reanalysis data were provided by the ECMWF data server.

University of East Anglia
Jessica Vial
j.vial@uea.ac.uk